

## Coupled Plasmas

W. Ebeling\*, J. Ortner

Institute of Physics, Humboldt University Berlin,  
Invalidenstr. 110, 10115 Berlin, Germany

**Abstract**

A survey on the dynamical and thermodynamical properties of plasmas with strong Coulomb interactions in the quasi-classical density-temperature region is given. First the basic theoretical concepts describing nonideality are discussed. The chemical picture is introduced. It is shown that the nonideal plasma subsystem of the free charges has a rather large quasi-classical regime, where the quantum effects yield only corrections to the merely classical dynamics. The plasma of free charges may be described by effective potentials which incorporate quantum effects in an approximative way. The simplest effective potentials are only space-dependent, more advanced methods include momentum-dependent interactions. On the basis of these potentials analytical results are derived and simulation methods are developed. It is shown that effective potentials are appropriate for the description of thermodynamical as well as collective properties.

PACS: 52.65.-y, 71.45.Gm, 03.65.Sq, 05.30.Fk

## 1 Introduction

Strongly coupled plasmas play an important role in nature, laboratory experiments, and in technology [1, 2, 3, 4]. In these plasmas the mean potential energy is of the same order of magnitude as the mean kinetic energy. Then we speak also about nonideal plasmas. We will study in this work the dynamics, thermodynamic properties and several collective effects of strongly coupled non-degenerate one-component plasmas (OCP) and symmetrical two-component plasmas (TCP). The investigation is restricted to the subsystem of the free charges, which is defined by means of the chemical picture [2]. In this model the atoms, ions, and molecules are treated as separate species. Therefore the constituents of the plasma are free electrons, free nuclei, ions, atoms, and molecules. All species are treated on equal footing (principle of particle democracy).

---

\*email:werner@summa.physik.hu-berlin.de

The main purpose of this work is the investigation of a quasi-classical dynamics of free charges based on effective potentials which may be used to describe thermodynamical and collective properties of the free charges in this subsystem. We restrict ourselves to the classical and near-classical region. Degeneracy is taken into account only in an approximative way. Therefore the new results refer in particular to a region where the plasma is still nondegenerated but nevertheless strongly coupled [6]. In this work we will restrict ourselves to one-component plasmas and to two-component plasmas which are anti-symmetrical with respect to the charges ( $e_- = -e_+$ ) and symmetrical with respect to the densities ( $n_+ = n_i = n_- = n_e$ ). In particular we consider the model case of electron - positron plasmas  $m_+ = m_e$  and H-plasmas with the mass-relation  $m_+ = 1840 m_e$ . We include the - so far unrealistic - case of mass - symmetrical plasmas since in this case the thermodynamic functions and other analytic functions describing the plasma are of particular simplicity. This is due to cancellation effects caused by the symmetry of the masses and anti-symmetry of the charges [7]. The effective potentials may be used to calculate correlation functions, thermodynamic properties and structure factors of the free charges in semi-classical non-degenerate quantum plasmas. The effective potentials are first obtained from the Slater sum method. Then momentum-dependent potentials are introduced and discussed.

*Characteristic parameters:* The average distance of the electrons is the Wigner-Seitz radius  $d = [3/4\pi n_e]^{1/3}$ , the Bohr radius is defined as  $a_B = \hbar/me^2$ . Other characteristic lengths are the Landau length  $l = e^2/kT$ , the De Broglie wave-length  $\Lambda_i = h/[2\pi m_i kT]^{1/2}$  of particles of species  $i$  and thermal wave length of relative motion  $\lambda_{ij} = \hbar/(2m_{ij}kT)$ . Furthermore we define the following dimensionless parameters:

- (i) the coupling strength:  $\Gamma = l/d$ .
- (ii) the degeneration parameter:  $n_i \Lambda_i^3$  or  $\theta = 2mkT/[\hbar^2 (3\pi^2 n_e)^{2/3}]$ .
- (iii) the interaction parameter  $\xi_{ij} = -(e_i e_j)/(kT \lambda_{ij})$ .

Let us first discuss the OCP: In the limit when the average distance is large in comparison with the Bohr radius, i.e. if  $d \geq a_B$  the electron gas behaves classical. The classical case was treated analytically by Abé and others [8], Monte Carlo calculations in a wide range of  $\Gamma$ -values were carried out e.g. by Brush, Sahlin and Teller, DeWitt, Ichimaru and other workers (see [9, 1, 3, 4]). Quantum corrections to the classical case which are relevant at moderate values of  $r_s$  were investigated by many authors [1, 10, 11]. All the analytical calculations mentioned so far cover only limiting cases as e.g.  $r_s < 1$  or  $\Gamma < 1$ . This is the reason why simulations are of large interest. There exists extensive Monte Carlo (MC) calculations for the classical region [12]. Classical molecular dynamics (MD) calculations were presented by Hansen et al. [13]. The particular interest in MD calculations is connected with the fact, that they give

the analytically accessible regions. Further we mention several investigations devoted to the simulation of two-component plasmas [18, 19, 20, 21, 25, 28]. In particular our interest is devoted here to quasi-classical methods. Quasi-classical simulations of two-component plasmas were pioneered by Norman and Hansen [18, 19]. These methods attracted a great deal of interest because of their relative simplicity. A special direction in developing simulation methods uses momentum-dependent potentials. The main idea in this approach is to model quantum effects by certain constraints in the phase space constructing an appropriate Hamiltonian [22, 23, 24]. In particular the Pauli exclusion principle is simulated by a momentum-dependent two-body interaction.

## 2 Effective Interaction Potentials

### 2.1 Space - Dependent Effective Interactions

As pointed out the idea of quasi-classical methods is to incorporate quantum-mechanical effects (in particular the Heisenberg and the Pauli principles) by appropriate potentials. Such a quasi-classical approach has of course several limits which are basically connected with the trajectory concept. We mention for example the principal difficulty to describe microscopic quantum effects as tunnelling, and macroscopic quantum effects as superfluidity and superconductance. Our aim is only the calculation of standard macroscopic properties which have a well defined classical limit. Since bound states cannot be described classically our methods are restricted to the subsystem of free charges. However, this is not a very serious restriction since most of the plasma properties are determined by the subsystem of the free charges.

The easiest way to arrive at effective potentials describing quantum effects is the use of the so-called Slater sums which are defined by the  $N$  - particle wave functions,

$$S(\mathbf{r}_1, \dots, \mathbf{r}_N) = \text{const} \sum \exp(-\beta E_n) |\Psi_n(\mathbf{r}_1, \dots, \mathbf{r}_N)|^2 \quad . \quad (1)$$

The integrals over the distributions  $S(\mathbf{r}_1, \dots, \mathbf{r}_N)$  yield the correct quantum statistical partition function. The Slater sums for Coulombic systems were studied in detail by several authors [1, 6]. With the knowledge of the Slater sums one gets exact space distributions in equilibrium by the choice

$$U^{(N)}(\mathbf{r}_1, \dots, \mathbf{r}_N) = -kT \ln S(\mathbf{r}_1, \dots, \mathbf{r}_N) \quad . \quad (2)$$

These potentials are often called quantum statistical effective potentials and they are used to calculate the partition function [1, 6, 18]. Thus one obtains the correct

degenerate region.

The Slater sum is an analogue of the classical Boltzmann factor and one defines therefore an effective potential by

$$S_{ab}^{(2)}(r) = \exp(-\beta u_{ab}(r)) = \text{const.} \sum_{\alpha} \exp(-\beta E_{\alpha}) |\Psi_{\alpha}|^2 . \quad (3)$$

Here  $\Psi_{\alpha}$  and  $E_{\alpha}$  denote the wave functions and energy levels of the pair  $ab$ .

A quantum mechanical calculation including the first orders in the perturbation theory was first given by Kelbg; a similar more simple effective potential was derived by Deutsch and was used in the simulations by Hansen and McDonald [19].

The effective potentials derived from perturbation theory do not include bound state effects. In order to treat the region, where bound states are of importance, a quite different approach is necessary [6]. The first step is a transition to the chemical picture i.e. bound and free states have to be separated. The second step is the derivation of an effective potential for the interaction of the free charges in the plasma. In order to proceed we split the Slater sum into a bound part and a free part. This splitting is not unique. We use here the so - called Brillouin - Planck - Larkin (BPL) convention. This way of division free - bound corresponds to a smooth cut - off of the partition function which is based on omitting of the divergent elements in the sum. This leads to [1]

$$S_{ab}^b(r) = \text{const.} \sum'_{\alpha} (\exp(-\beta E_{\alpha}) - 1 + \beta E_{\alpha}) |\Psi_{\alpha}|^2 , \quad (4)$$

where the sum extends only over all the discrete states. It is well known, that the BPL - convention leads to the simplest expressions for the thermodynamic functions. The Slater sum of the free charges is defined by [1, 5, 6]:

$$S_{ab}^*(r) = S_{ab}^{(2)} - S_{ab}^b = \exp(-\beta u_{ab}^*(r)) . \quad (5)$$

In this way we arrive at an effective interaction potential of the free particles  $u_{ab}^*(r)$ , which is finite for  $\hbar \neq 0$  and has a weak (integrable) singularity in the limit  $\hbar \rightarrow 0$ .

For the electron - electron and for the ion - ion interaction the classical limit gives simply the Boltzmann factors, i.e.  $u_{ee}^* = u_{ii}^* = e^2/r$ . For the electron - ion pairs one has to perform the classical limit in eq.(5). Explicitly one finds for the classical limit within the BPL - convention [6, 4]:

$$\begin{aligned} S_{ei}^*(r) = & \exp\left(\frac{Ze^2}{kTr}\right) \cdot \left[1 - \Phi\left(\sqrt{\frac{Ze^2}{kTr}}\right)\right] + \frac{2}{\sqrt{\pi}} \sqrt{\frac{Ze^2}{kTr}} \\ & + \frac{4}{3\sqrt{\pi}} \left(\frac{Ze^2}{kTr}\right)^{3/2} + \frac{8}{15\sqrt{\pi}} \left(\frac{Ze^2}{kTr}\right)^{5/2} , \end{aligned} \quad (6)$$

may be used for simulations of the free charges in the purely classical region.

## 2.2 Momentum - Dependent Effective Interactions

As mentioned already above, a principal disadvantage of purely space-dependent potentials is the incorrect representation of the momentum - distributions of the plasma. In order to achieve a correct representation of the Fermi distribution for the momenta, momentum-dependent potentials have to be included [23, 25, 27]. In what follows we will assume a quasi-classical Hamiltonian of the following structure:

$$H = \sum_{i=1}^N \frac{p_i^2}{2m} + \sum_{i<j} V_P \left( \frac{r_{ij}}{r_{ij0}}, \frac{p_{ij}}{p_{ij0}} \right) + \sum_{i<j} \frac{e^2}{r} \cdot F \left( \frac{r_{ij}}{r_{ij0}}, \frac{p_{ij}}{p_{ij0}} \right) \quad . \quad (8)$$

Here  $r_{ij}$  is the usual distance in the coordinate space and  $p_{ij}$  the distance in the momentum space. Further we define the characteristic parameters

$$r_{ij0}^2 = r_{i0}^2 + r_{j0}^2; \quad p_{ij0}^2 = p_{i0}^2 + p_{j0}^2; \quad p_{i0} = \hbar/r_{i0} \quad , \quad (9)$$

where  $r_{i0}$  is a characteristic length (i.e., the radius of the wavepacket) of the particle  $i$ . We have in the Hamiltonian two kinds of particle interaction: the so-called Pauli-potential  $V_P$  acting only between identical particles and a Coulomb interaction modified by a certain function  $F(x, y)$ . In order to derive effective expressions of this type the Hamilton operator  $\hat{H}$  is averaged with respect to test wave functions [25],

$$H(q, p; \hbar) = \int d\mathbf{x} \psi_o^*(x) \hat{H} \psi_o(x) \quad . \quad (10)$$

This definition of an effective Hamiltonian stems from the so-called wave-packet dynamics. In the last time it has found several applications to plasmas [25, 26, 29, 30]. If one chooses for the test wave functions symmetrized and anti-symmetrized combinations of minimum uncertainty wave packets for the particles of species  $k$ ,

$$\psi_{k0}(x) = \text{const} \exp \left( -\frac{(x-q)^2}{2r_{k0}^2} + \frac{ipx}{\hbar} \right) \quad , \quad (11)$$

one does not get any Pauli potential for two electrons with antiparallel spins, for two electrons with parallel spins the following Pauli potential is obtained,

$$V_{P_{ij}}(x, y) = \delta_{ij} \frac{\hbar^2}{mr_{ij0}^2} \exp \left( -\Delta^2 \right) \frac{\Delta^2}{1 - \exp(-\Delta^2)} \quad . \quad (12)$$

This is a two-body interaction depending on the phase-space distance  $\Delta^2 = x^2 + y^2$ . In our simulations we averaged over the two spin configurations and used a simplified Pauli-Potential which is purely Gaussian [23],

described by the function  $F$  (eq. 8). We obtain

$$F(x, y) = \text{erf}(x) \quad . \quad (14)$$

This potential was obtained already by Klakow et al. [25], it represents the electrostatic energy between two charges which are Gauss-distributed. The free potential parameter  $r_0$  was fitted in such a way, that the properties of an electron gas without interactions as the binary correlation function and the Fermi momentum distribution are well reproduced. We assume that the momentum uncertainty is given by that of the free Fermi gas. In this way we get

$$p_{i0}^2 = \frac{4}{3} m \epsilon_{kin}^{(i)} \quad (15)$$

and  $r_{i0} = \hbar/p_{i0}$ , where  $\epsilon_{kin}^{(i)}$  is the mean kinetic energy of the free Fermi gas of particles of species  $i$ . These relations yield at high temperatures  $p_{i0}^2 = m_i kT$ ;  $r_{i0} = 2r_{i0}^2 = \hbar^2/2m_i kT = \lambda_{ii}^2/2$ ;  $V_0 = kT/2$ . We mention that there exist other estimates for the free parameters of the Pauli-potential [23].

### 3 Quantumstatistical Theory and Simulations

#### 3.1 Thermodynamic Properties

Quantum corrections to the classical electron gas were derived in earlier work [10, 27]. Generalizing the methods developed earlier [27] to the case of the TCP we assume that the interaction part of the free energy density of the plasma can be split into a classical and a quantum-mechanical part

$$f_{int} = f_{cl} + f_{qu} \quad , \quad (16)$$

where  $f_{cl}$  is the known free energy density of the classical plasma of free charges and  $f_{qu}$  is the difference between the full and the classical free energy density. Explicit calculations for the classical free energy of the electron gas were given first by Abé for the low density case and extended by Cohen and Murphy [8]. For a symmetrical classical TCP it was shown that (with the BPL convention) the first correction beyond the Debye term in the density expansion of the free energy vanishes. [5].

Consider now the quantum-mechanical corrections to the classical free energy density. For the plasma of free charges this expression is convergent. In the low density limit we get

$$f_{qu} = -kT \sum n_i n_j \delta B_{ij}(T) \quad . \quad (17)$$

over the resolvent of the Coulomb scattering problem. For a mass-symmetrical TCP all terms except to one cancel and we get (neglecting exponentially small degeneracy effects) the rather simple result

$$f_{qu} = -\pi^{3/2} n_i n_e \lambda_{ie}^3 \xi_{ie}^2 + O(n^{3/2}) \quad (18)$$

If the masses are not symmetrical, infinite series in the  $\xi$  - parameter appear, the so-called quantum virial functions  $Q$  and  $E$  [1, 6]. The theory may be extended to higher concentration by using the method of Padé - approximations [7].

We carried out extensive simulations for the electron gas [27] and also a few simulations for the symmetrical TCP by using the effective Hamiltonian described above. Since our modified Coulomb interaction differs from the bare Coulomb interaction only for short distances the Ewald sum technique for handling the long range part could be used. To study equilibrium properties, as e.g. the average energy we carried out several Monte Carlo runs of  $2 \cdot 10^6$  steps for ensembles of 64-512 particles. The results were extrapolated to infinite particle numbers. The regions of degenerate and nondegenerate plasmas were investigated. The results of our simulations were discussed in detail in earlier work [27, 28]. As the main result we may quote, that at all densities the deviations from the classical calculations are very small [28]. Further we may state that the overall agreement between the analytical formulae and the simulations is rather good. The deviations are all within the error bars of the simulations. Only at low temperature a systematic deviation is observed, here the semi - classical model does not work. At conditions of weak or moderate degeneracy our model yields quite reasonable results.

### 3.2 Collective Excitations

In order to study collective nonequilibrium effects we simulated a system of 250 electrons with periodic boundary conditions by Molecular Dynamics (MD) calculations. Usually MD simulations consist of two parts: First the desired temperature is adjusted using some thermostat, while in a second phase the energy is kept constant and measurements are performed. Since most known thermostats do not work in the case of momentum dependent interactions we replaced the equilibration phase by a MC simulation using the Metropolis Algorithm. This Algorithm is independent from any particular form of the interaction. To perform the MD simulations we used a 4th order Runge-Kutta integrator with stepsize control. The runs were of length of order 1000 times the inverse plasma frequency.

First the individual motion of the electrons was studied by calculating the velocity autocorrelation function  $\langle v(t + \tau)v(t) \rangle_t$  [27, 30]. It was shown that for moderate

To describe the collective behavior of the system we have investigated the dynamic structure factor of the electron system,

$$S(\vec{k}, \omega) = \frac{1}{2\pi N} \int_{-\infty}^{\infty} e^{i\omega t} \langle \rho(\vec{k}, t) \rho(-\vec{k}, 0) \rangle dt \quad , \quad (19)$$

where  $\rho(\vec{k}, t) = \sum_i \exp(-i\vec{k}\vec{r}_i)$  is the Fourier component of the microscopic electron density. We obtained the dynamic structure factor from the MD simulations by approximating the Heisenberg operator  $\vec{r}_i(t)$  by the position of the  $i$ -th particle in the simulations. However, the thus obtained quantity (we denote it by  $R(\vec{k}, \omega)$ ) is symmetric with respect to the frequency. It corresponds therefore to a classical fluctuation-dissipation theorem,

$$R(\vec{k}, \omega) = (n\pi\phi(k)\beta\omega)^{-1} \text{Im} \varepsilon^{-1}(\vec{k}, \omega) \quad . \quad (20)$$

where  $\varepsilon(\vec{k}, \omega)$  is the dielectric function of the electron OCP. It can be seen from Eq. (20) that  $R(\vec{k}, \omega)$  cannot be regarded as a structure factor, but as a normalized loss function. In what follows we will discuss the normalized loss function. Notice, that in the classical case the loss function and the dynamic structure factor coincide.

We have plotted the loss function  $R(q, \omega)$  ( $q = ka$ ) for various  $q$  values, for the case of moderate coupling ( $\Gamma = 1$ ), strong coupling ( $\Gamma = 10$ ) and for the case of very strong coupling ( $\Gamma = 100$ ) and for different parameters of degeneracy  $\theta = 1$  (moderate degenerate) and  $\theta = 50$  (classical plasma) (Figs. 1-6). For the regime of moderate coupling we have compared the results of the simulations with the corresponding data from the Random Phase approximation (RPA), [30]. We see from Figs. 1, 2 that in the case of a moderate coupled plasma ( $\Gamma = 1$ ) the shape of the loss function calculated from the simulations is damped stronger and slightly shifted to the left in comparison with the RPA loss function. For moderate coupling and in both cases (weakly degenerate and classical plasma) the plasmon peak can be observed only for the smallest  $q$  value ( $q=0.619$ ). From Figs 1 and 2 it can be also seen that the change of the degeneracy parameter  $\theta$  in the range from 50 to 1 has only a small influence on the results.

However, at higher degrees of degeneracy ( $\theta = 0.15$ ) the plasmon peak obtained from the MD datas is shifted towards higher frequencies. But the peak position in this case differs quite significantly from those predicted by the RPA which is shifted much more due to the increase of the average velocity (the Fermi velocity) which leads to a strong positive dispersion (Fig. 3). The simulations underestimate this shift.

In the strong coupling regime ( $\Gamma = 10$ ) and for a moderate degenerate plasma ( $\theta = 1$ ) we observed at the smallest  $q$  value a sharp plasmon peak centered near  $\omega_P$  (Fig. 4). With the increasing wavevector the plasmon peak widens, a plasmon peak



region from positive (at smaller  $\Gamma$ ) to negative dispersion (at higher  $\Gamma$ ).

In the case of very strong coupling  $\Gamma = 100$  an extremely sharp plasmon peak centered near  $\omega_P$  can be observed at the smallest  $q$  value (Figs. 5, 6). Here the plasmon peak can be observed up to  $q = 3.094$ . For both the case of a classical plasma ( $\theta = 50$ ) and for the case of moderate degenerate plasma ( $\theta = 1$ ) a negative dispersion is seen (with increasing wavenumber the peak position is shifted more and more to the left). This behavior contradicts to the RPA where no plasmon peak is predicted in this regime due to the strong Landau damping. However, the RPA cannot be applied to the strong coupling regime. On the contrary, the results of our simulations for the case of a weakly degenerate plasma ( $\theta = 50$ ) are in a good agreement with the results of corresponding MD simulations of Hansen et al. for the classical one component plasma [13]. From Figs. 5 and 6 one also sees that the negative dispersion is more pronounced in the case of a classical plasma.

Further we have compared the results of our simulations with the expression of the dynamic structure factor obtained by the application of the classical theory of moments which is appropriate also for the case of strong coupling [31]. A more detailed discussion can be found elsewhere [30]. Here we show the results for two different  $q$  vectors at  $\Gamma = 100$  (Figs. 7, 8 [30]). The agreement of the loss functions calculated by the application of the theory of moments (sum rules approach) with that from the MD calculations is rather good. The theoretical curves reproduce the varying shape of the dynamic structure factor and describe the plasmon peak position in a satisfactory manner. However, the agreement in the height of the peaks is less satisfactory.

Thus we can conclude that due to the quasi-classical character our quantum molecular dynamic simulations describe the collective excitations of the electron gas only approximately. Our model yields quite reasonable results at weak and moderate degeneracy, whereas for the case of high degeneracy it seems to break down.

## 4 Discussion

We developed here a simple quasi-classical model of quantum plasmas based on a dynamics with an effective momentum-dependent Hamiltonian. The quantum-mechanical effects corresponding to the Pauli and the Heisenberg principle were modeled by constraints in the Hamiltonian. By using the concept of minimum uncertainty wave packets, momentum-dependent effective potentials were derived. The effective potentials were used to simulate one-component plasmas and mass-symmetrical two-component plasmas by means of MC and MD methods. The result of the simulations is in good agreement with analytical calculations of the thermodynamic properties in the region of small degeneracy and moderate coupling.

analytical theory based on RPA, sum rules and the theory of moments is reasonable. In most cases the shape and the location of the plasmon peak is reproduced in a reasonable way, in some cases larger deviations are observed. We cannot expect however, that the present model, which was obtained by fitting the potential to equilibrium properties will describe all non-equilibrium properties in a quantitative way. Further improvements of the model might be unavoidable. We may hope however that at least near to equilibrium some realistic features are still reflected by the model.

Acknowledgment: The authors thank V.M. Adamyan, Yu.M. Klimontovich, B. Militzer, V. Podlipchuk and I.M. Tkachenko for helpful discussions.

## References

- [1] Kraeft, W.D., Kremp, D., Ebeling, W. and Röpke, G., “Quantum Statistics of Charged Particle Systems”. (Akademie-Verlag, Berlin; Plenum Press, New York; russ. transl: Mir, Moscow 1986).
- [2] Ebeling, W., Förster, A., Fortov, V.E., Gryaznov, V.K. and Polishchuk, A.Ya., “Thermophysical Properties of Hot Dense Plasmas” (Teubner, Stuttgart-Leipzig 1991).
- [3] Ichimaru, S. “Statistical Plasma Physics: I. Basic Principles, II: Condensed Plasmas”. (Addison-Wesley, Reading, 1992, 1994).
- [4] Kraeft, W.D. and Schlages, M. (editors), “Physics of Strongly Coupled Plasmas” (World Scientific. Singapore, 1996).
- [5] Ebeling, W., Ann. Physik, **19**, 104 (1967).
- [6] Ebeling, W., Ann. Physik, **21**, 315 (1968); **22** (1969) 33,383,392; Physica **38**, 378 (1968); **40**, 290 (1968); **43**, 293 (1969); **73**, 573 (1974).
- [7] Lehmann, H. and Ebeling, W., Phys. Rev. E, **54**, 2451 (1996).
- [8] Cohen, E.G.D. and Murphy, T.J., Phys. Fluids **12**, 1404 (1969).
- [9] March, N.H. and Tosi, M.P., “Coulomb Liquids”. (Academic Press, London, 1984).
- [10] Hoffmann, H.J. and W. Ebeling, W., Physica, **39**, 593 (1968).
- [11] Deutsch, C. and Lavaud, M., Phys. Lett., A **39**, 253 (1972); **43**, 193 (1973).

- [13] Hansen, J.-P., McDonald, I.R. and Pollock, E.L., Phys. Rev. A **11**, 1025 (1975).
- [14] Ceperley, D.M. and Alder, B.J., Phys. Rev. Lett, **45** 7, (1980).
- [15] Ebeling, W., Kraeft, W.D. and D. Kremp, D., Contr. Plasma Phys., **10**, 237 (1970).
- [16] Alastuey, A., Cornu, F. and Perez, A., Phys. Rev. E, **49**, 1077, (1994).
- [17] Ebeling, W., Contr. Plasma Phys., **30**, 553 (1990); **33**, 492 (1993).
- [18] Zamalin, V.M., Norman, G.E. and Filinov, V.S., “The Monte Carlo Method in Statistical Mechanics” (in Russ.) (Nauka, Moscow, 1977).
- [19] Hansen, J.-P. and McDonald, I.R., Phys. Rev. ,A **23**, 2041, (1981).
- [20] Penman, J.I., Clerouin, J. and Zerah, P.G., Phys. Rev E, **51**, R5224, (1995).
- [21] Pierleoni, C., Ceperley, D.M., Bernu, B. and Magro, W.R., Phys. Rev. Lett., **73**, 2145, (1994).
- [22] Heller, E.J., J. Chem. Phys., **62**, 1544, (1975).
- [23] Dorso, C. and Randrup, J., Phys. Lett. B, **215**, 611, (1988).
- [24] Feldmeier, H., Bieler, K. and Schnack, J., Nucl. Phys. ,A **586**, 493, (1995).
- [25] Klakow, D., Toepffer, C. and Reinhard, P.-G., Phys. Lett. A, **192**, 55, (1994); J. Chem. Phys., **101**, 10766, (1994).
- [26] Ebeling, W. and Militzer, B., Phys. Lett. A, **226**, 298 (1997).
- [27] Ebeling, W. and Schautz, F., Phys. Rev E, **56**, 3498 (1997).
- [28] Ebeling, W., Militzer, B. and Schautz, F., Contr. Plasma Phys. **30** 553 (1997).
- [29] Ebeling, W., Forster, A. and Podlipchuk, V., Phys. Lett. A, **218**, 297 (1996).
- [30] Ortner, J., Schautz, F. and Ebeling, W., Phys. Rev E, **56**, 4665 (1997).
- [31] Adamyan, V.M. and Tkachenko, I.M., High Temp. (USA) **21**, 307 (1983)); see also Ortner, J. and Tkachenko, I.M., Phys. Rev. A **46**, 7882 (1992).

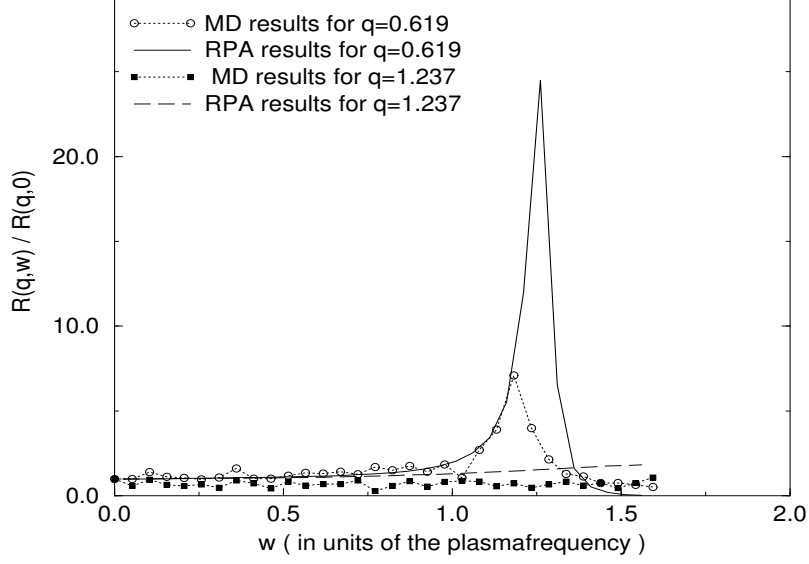


Figure 1: Comparison of the MD and RPA loss function  $R(q, \omega)$  versus frequency  $\omega/\omega_p$  for different wavevectors  $q$  at  $\Gamma = 1$  and  $\theta = 1$ , [30] .

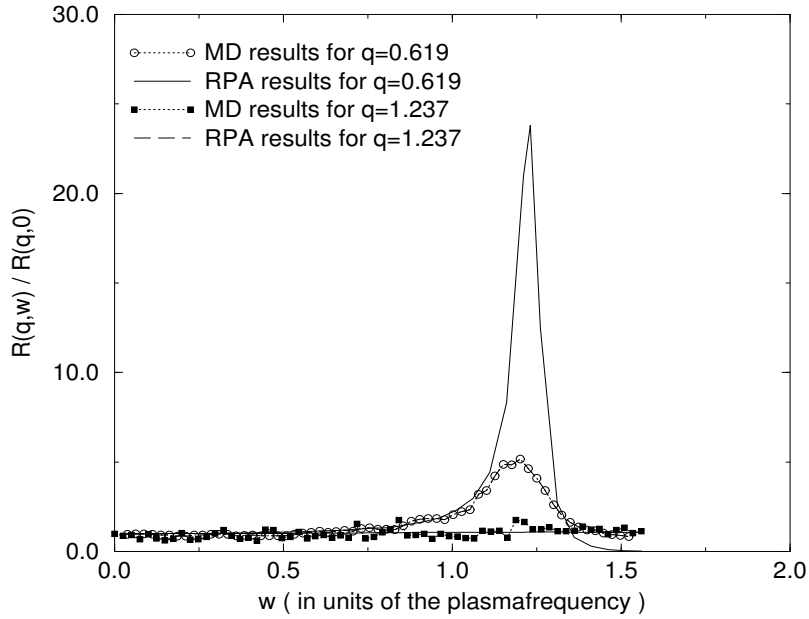


Figure 2: same as Fig. 1; for  $\Gamma = 1$  and  $\theta = 50$ , .

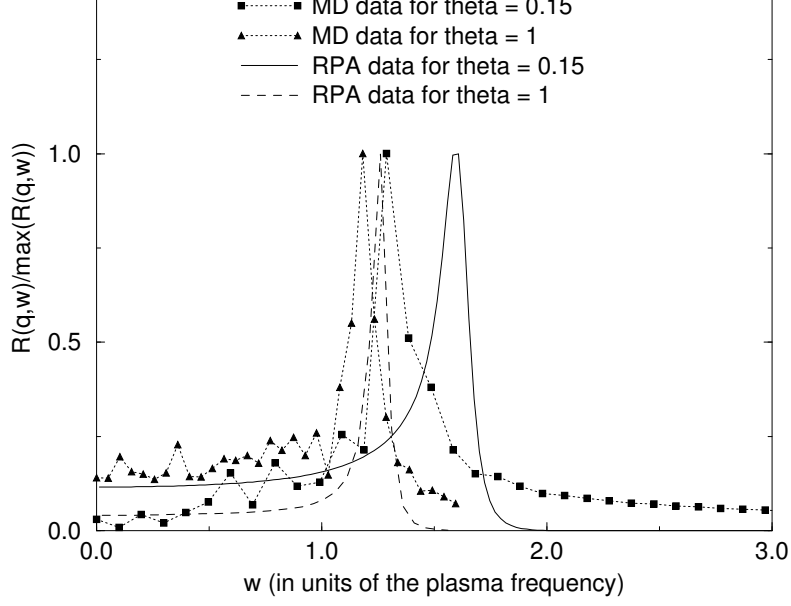


Figure 3: The MD loss function  $R(q, \omega)$  versus frequency  $\omega/\omega_p$  for wavevector  $q = 0.619$  at fixed  $\Gamma = 1$  and different  $\theta$ .

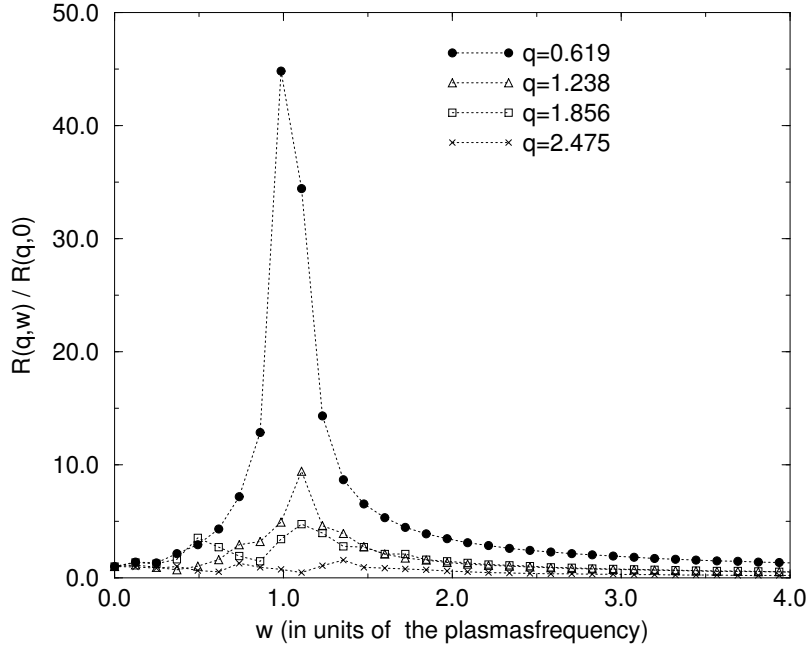


Figure 4: The MD loss function  $R(q, \omega)$  versus frequency  $\omega/\omega_p$  for different wavevectors  $q$  at  $\Gamma = 10$  and  $\theta = 1$ .

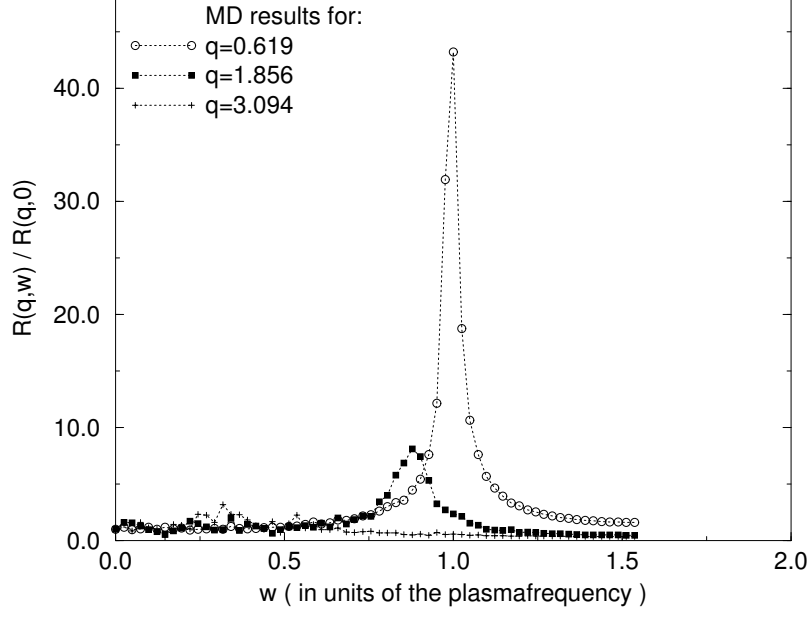


Figure 5: The MD loss function  $R(q, \omega)$  versus frequency  $\omega/\omega_p$  for different wavevectors  $q$  at  $\Gamma = 100$  and  $\theta = 50$

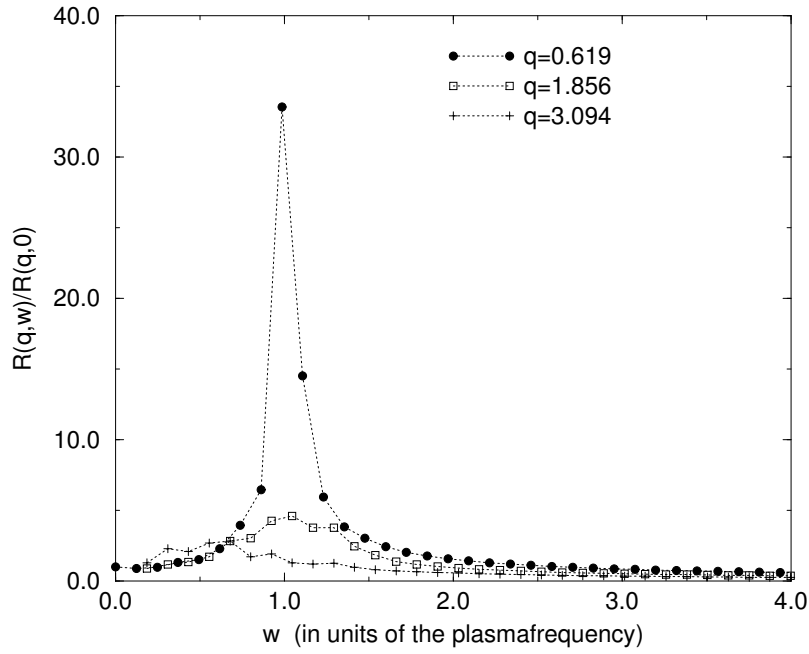


Figure 6: same as Fig. 5, at  $\Gamma = 100$  and  $\theta = 1$ .

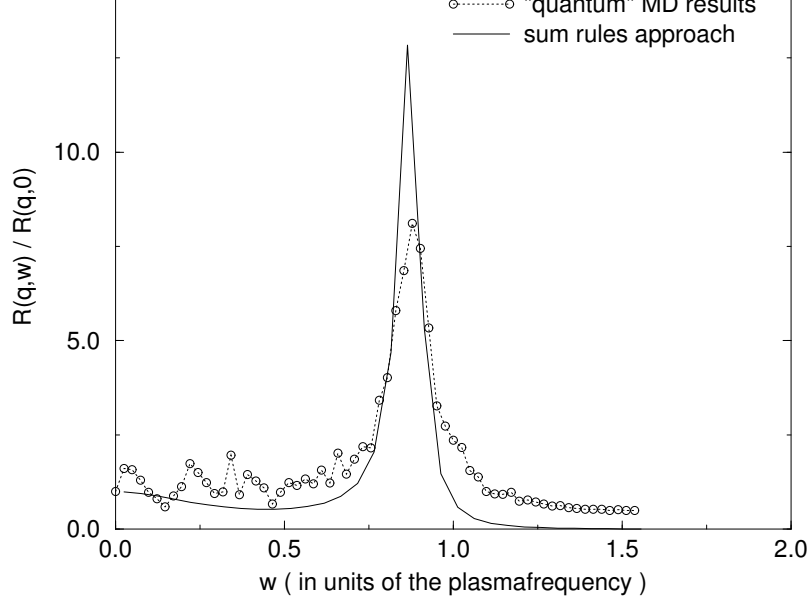


Figure 7: comparison of the MD loss function  $R(q, \omega)$  versus frequency  $\omega/\omega_p$  with the corresponding loss function from the sum rules approach at  $\Gamma = 100$  and  $\theta = 50$  for wavevector  $q = 1.856$ , .

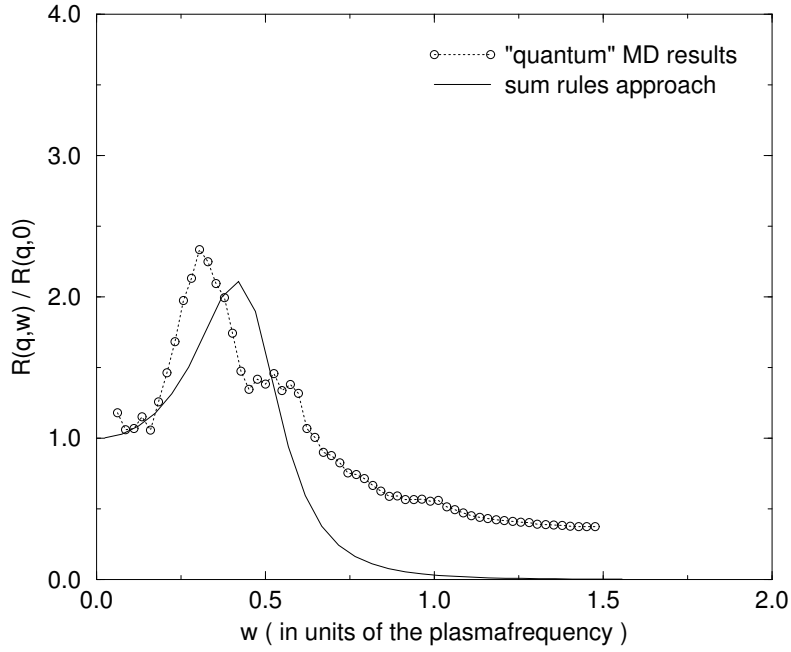


Figure 8: same as Fig.7; at  $\Gamma = 100$  and  $\theta = 50$  for wavevector  $q = 3.094$ , .